respectively. We would like to emphasize however, that while looking at the temperature dependence of the EDS contribution, one should keep in mind the restricted temperature range (~30–80°K) for which the theory is applicable.

In the general case, it is difficult to state the explicit dependences of the NP and EDS contributions on temperature. However, in the case when the EDS contribution is a small correction to the NP contribution, one may be able to distinguish between the two, by noticing from the analysis that the temperature dependence of EDS contribution is close to the temperature dependence of NP contribution multiplied by the temperature dependence of $(\omega_2\tau_0)^{-1}$. Thus the dominant scattering mechanism determines the distinction between the temperature dependences of NP and EDS contributions.

Wynne[5] has recently carried out an interesting experimental investigation on optical mixing in GaAs, Ge, Si, and InAs and has drawn some very useful conclusions about the nonparabolicity of the conduction band in GaAs. He has however, summarily rejected the EDS mechanism of optical mixing in his paper. It is quite conceivable that the parameter range of his experiments (especially the low carrier concentration) is such that the EDS contribution is actually negligible. However, it is quite clear that if one goes to a different parameter range (such as the one studied in this paper), then the EDS contribution may become comparable to the NP contribution and one will have to take it into account to draw correct conclusions about band nonparabolicity.

We conclude, finally, that optical mixing by free carriers in semiconductors may contain comparable contributions from conduction-band nonparabolicity and an energy-dependent scattering time.

ACKNOWLEDGMENTS

The authors are grateful to Dr. J. Dawson for critically reading the manuscript. This work was performed partially under the auspices of the U. S. Atomic Energy Commission, Contract No. AT(30-1)-1238, and partially supported by the Environmental Science Services Administration.

PHYSICAL REVIEW B VOLUME 1, NUMBER 8 15 APRIL 1970

Photoelectric Emission from Silicon

R. M. Broudy
United Aircraft Research Laboratories, East Hartford, Connecticut 06108
(Received 11 October, 1968; revised manuscript received 2 May 1969)

Effects of band structure on photoelectric yields from silicon have been determined from the interpretation of measurements which were made on surfaces oriented perpendicular to (111), (110), and (100). It was established that the yield spectrum for properly polished and annealed silicon is the same as that for cleaved and annealed silicon; low-energy electron diffraction patterns were obtained for all surfaces. Photoelectric thresholds obtained for (111), (110), and (100) silicon were 4.60, 4.73, and 5.11 eV, respectively. Improved experimental procedures show that yields well above threshold vary more rapidly with photon energy than those previously observed. Crystallographic differences in yields near threshold are ascribed to two sources: (1) the ionization energy ξ, which represents surface-barrier energy, and (2) the additional energy E_A required to emit electrons with crystal momentum ($\mathbf{k}$) at an angle θ to the surface normal, beyond that for $\mathbf{k}$ at $\theta=0$. It is shown that for transitions near the center of the Brillouin zone (BZ), E_A can be quite small (~0.15 eV); hence, electrons at large θ can be emitted for $h\nu-h\nu_0$ only a few tenths of an eV, where $h\nu_0$ is the threshold photon energy. For $(h\nu-h\nu_0)>1.0$ eV, electrons are emitted for all θ, i.e., for all excitation within the inner half of the BZ. A quantitative estimate of crystallographic yield dependence gives good agreement for the assumption, suggested by the band structure, of transitions near threshold peaked for $\mathbf{k}$ along $\langle 111\rangle$. These considerations lead to a more accurate interpretation of Y versus $(h\nu-h\nu_0)$, which depends on the position in the BZ of the operant optical transition. Such effects must be considered in analyzing all photoemission experiments, including both yield and energy distribution measurements.

I. INTRODUCTION

In terms of one-electron solid-state theory, the volume photoelectric process consists of three stages: (1) excitation of an electron to an upper energy band by absorption of electromagnetic radiation; (2) motion of "hot carriers" in the upper band with elastic and inelastic scattering; (3) emission through the potential barrier at the surface of those electrons which have sufficient energy and the proper crystal momentum. Investigators interested in band structure information concentrate on stage 1 generally by measuring energy distribution of emitted electrons[1]; those interested in surface barriers concentrate on stage 3 generally by measuring total photoelectron yield versus photon energy.[2]

[1] Typical recent papers are J. L. Shay and W. E. Spicer, Phys. Rev. **161**, 799 (1967); T. A. Callcott, *ibid.* **161**, 746 (1967); T. E. Fischer, *ibid.* **147**, 603 (1966); F. G. Allen and G. W. Gobeli, *ibid.* **144**, 558A (1966).

[2] Some typical papers are J. van Laar and J. J. Scheer, Surface Sci. **3**, 189 (1965); F. G. Allen and G. W. Gobeli, Phys. Rev. **127**, 150 (1962); J. van Larr and J. J. Scheer, Philips Res. Repts. **17**, 101 (1962); J. A. Dillon, Jr., and H. E. Farnsworth, J. Appl. Phys. **29**, 1195 (1958).

It is not usually possible to separate completely the stages of photoemission in a simple manner since all photoelectrons experience all three stages. The present work, which is devoted to spectral yield measurements provides an explanation of the role of band structure in photoelectric yields from silicon and resolves some previous difficulties in the interpretation of the photoemission process. It is shown that band-structure knowledge is required to determine surface potential barriers.

For semiconductors it is almost essential that such emission measurements, in addition to work function data, be used to determine potential energy barriers at surfaces because work function experiments, such as those of the Kelvin type, which measure contact potentials, determine energy differences only between the vacuum level and the Fermi level at the surface, which differences (unlike metals) can include internal potentials in the volume. Surface barriers can be specified, for instance, in terms of the difference in energy between an electron at the top of the valence band at the surface and at rest just outside the surface (the "vacuum level"); this quantity has been defined[3] as the ionization energy, ξ.

The earliest reported work on clean single crystal silicon is that of Dillon and Farnsworth[2] who obtained work functions by the Kelvin contact potential method and relative photoelectric yields up to photon energies of only 5.5 eV for (111), (110), and (100) silicon, which was cleaned by ion bombardment and annealing. Allen[4] reported the results of Kelvin contact potential measurements on (111) and (100) silicon which was etched and then cleaned by flashing in vacuum at temperatures above 1550°K. Allen and Gobeli[5] have measured work function, photoelectric yield, and energy distributions for cleaved, heated, and sputtered (111) silicon. Previously they had determined photoelectric yield and work function of cleaved (111) silicon,[2] mainly in order to determine band bending due to changes in surface potential caused by surface states. Photoelectric spectral yields have been studied by van Laar and Scheer[2] on silicon surfaces which were obtained by breaking in vacuum. Fischer[3] has determined positions of the Fermi level at the surface as well as work function differences between degenerate p- and n-type cleaved silicon by analysis of high- and low-energy limits of photoelectric energy distributions.

II. EXPERIMENTAL PROCEDURES AND ARRANGEMENTS

The silicon single-crystal samples of size approximately $\frac{1}{2}\times\frac{1}{2}\times 0.020$ in. were mounted on a molybdenum block and lightly held in place by a surrounding molybdenum shield with an opening approximately $\frac{3}{8}\times\frac{3}{8}$ in. to allow illumination and observation. All molybdenum parts were treated before use by vacuum heating to 1700°C for $\frac{1}{2}$ h. The molybdenum block was heated by radiation from an internal coil. The whole assembly was held in position on a stainless steel yoke by molybdenum hardware and sapphire insulation. A molybdenum heat shield was mounted between the molybdenum block and the yoke. This arrangement permitted heating the block well above 1100°C while maintaining the maximum temperature of the yoke below 200°C. Sample temperatures were obtained using both infrared and standard optical pyrometers. In the same experimental chamber was a Varian LEED optics unit which enabled monitoring of surface conditions by an independent method. The yoke which held the block and sample assembly was connected to a universal motion feedthrough which enabled positioning for both LEED and photoemission measurements.

Photocurrents leaving the sample were measured by a Cary vibrating reed electrometer. Contact was made to the block by a sapphire insulated wire. Leakage resistances were greater than $10^{14}\ \Omega$. The grids of the nearby LEED optics were used as an electron collector which was usually biased to 160 V; photocurrents were independent of bias above $\sim$40 V.

Ultraviolet illumination was obtained from a grating monochromator which was focused onto the sample through a quartz window. It was found that spurious currents due to generation of photoelectrons at the sample holder by reflected light could be minimized by tilting the sample slightly ($\sim 2°$) from the normal so that the reflected beam would strike the walls of the 18-in.-diam chamber and *not* emerge back through the window, which is the usual procedure. The magnitude of the spurious photocurrent was determined by measuring the spectral photoelectric yield with the sample insulated from the molybdenum holder, other experimental conditions being held identical. Appreciable corrections to measured data due to this effect were required only close to threshold for the (100) samples. The intensity of the monochromator output was obtained by reflecting the light from a front surface mirror (of calibrated reflectivity) to a Reeder quartz window uv type thermopile. Calibration was obtained with a standard lamp.

The data taken in the earlier stages of this work and shown in Fig. 1 were obtained with a Bausch and Lomb 500-mm grating monochromator illuminated with the standard Bausch and Lomb high pressure mercury lamp source. They are presented in order to permit comparison with previous work[5] which was performed under similar conditions.

Subsequently, it was found that yield data could be improved above about 5.8 eV and extended close to 6.5 eV (the uv air absorption limit) by several procedures which resulted in better spectral purity. They include the use of selected 200-W super pressure Xenon lamps for greater uv intensity, reduction of entrance and

[3] T. E. Fischer, Surface Sci. **10**, 399 (1968).
[4] F. G. Allen, J. Phys. Chem. Solids **8**, 119 (1959).
[5] F. G. Allen and G. W. Gobeli, J. Appl. Phys. **35**, 597 (1964).

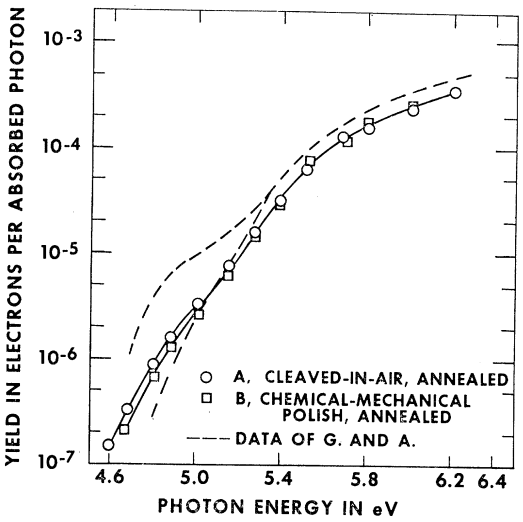

FIG. 1. Photoelectric yield in electrons per absorbed photon measured with standard system for (111) silicon surfaces. *A*, cleaved-in-air and annealed at 850°C 1 h in vacuum. *B*, chemical-mechanical polish and annealed at 850°C 1 h in vacuum. The dashed curves are the upper and lower limit given by Allen and Gobeli (Ref. 5) for cleaved-in-vacuum silicon—absolute accuracy ±100%.

exit slits from 1.0 to 0.50 mm, correction for and minimization of the effects of monochromator scattered light including provision that the light be focused parallel at the grating for each chosen wavelength. The principal effect of these techniques was found to be a lifting of the yield above about 5.8 eV.

All yields are given in terms of the absorbed energy which was determined from the reflectivity data of Philip and Taft.[6]

III. PHOTOELECTRIC YIELD—RESULTS OF SURFACE PREPARATION—COMPARISON WITH OTHER WORK

All samples were annealed at 850°C for 1 h at pressures less than 1×10^{-10} Torr in order to remove the thin oxide layer. For all methods of preparation discussed below, this was found sufficient to obtain an excellent quality Si(111) 7×7 LEED pattern.[7]

Silicon samples oriented within ±1° of (111) were prepared by several different methods: (1) routine metallographic polishing; (2) polishing and then etching in 1:1 HNO_3:HF; (3) polishing and etching in 1:1 HNO_3:HF followed by HF only; (4) chemical-mechanical polishing by standard semiconductor industry methods; (5) standard semiconductor industry silicon wafers were oxidized to a thickness of about 10 000 Å and the oxide was removed by immersion in HF; (6) finally, in order to compare the results with those for a surface which was not handled in any fashion, an *L*-shaped sample of the type described by Gobeli and Allen[8] was cleaved *in air* and introduced into the vacuum system with no further preparations.

All samples prepared by methods (4) to (6) gave the same spectral yield characteristics, except for a slight variability in the low energy spectrum, which agreed within experimental error with the data from the cleaved-in-air and annealed sample.[9] This is shown in Fig. 1, which shows the yield for a sample prepared by method (4), by method (6), and the results obtained by Allen and Gobeli[5] from samples which were cleaved-in-vacuum and annealed. Their observed low energy variability is indicated by the difference between the upper dashed line and the lower dashed line, which is their "low-energy limit." We have also observed similar low-energy variability, as shown by curve *A'* in Fig. 2, but not nearly so large. For samples prepared by methods (1)–(3), it was found that the spectral shape of the yield curves was similar to that of the other samples, but the absolute magnitude of the yield over the whole spectral range varied from sample to sample by as much as a factor of 2 from the smooth surface yields; hence they were not used.

For the satisfactory methods of preparation [methods (4)–(6)] spectral yields which did not change with subsequent annealing generally were obtained. Occasionally samples with erratic data were found; such samples never stabilized and the data were not used. As discussed above, the data presented in Fig. 1 (both ours and those of Allen and Gobeli[5]) were taken using the standard Bausch and Lomb system without improve-

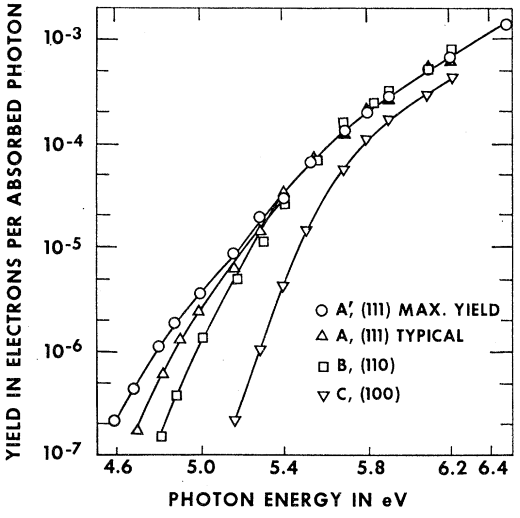

FIG. 2. Photoelectric yield in electrons per absorbed photon measured with improved system for silicon surfaces. *A'*, maximum low energy yield (111). *A*, typical (111); *B*, (110); *C*, (100).

[6] H. R. Phillipp and E. A. Taft, Phys. Rev. **120**, 37 (1960).
[7] J. J. Lander and J. Morrison, J. Appl. Phys. **34**, 1403 (1963).
[8] G. W. Gobeli and F. G. Allen, J. Phys. Chem. Solids **14**, 23 (1960).
[9] The excellent results from semiconductor industry silicon are not unexpected since the technology evolved in response to stringent requirements on surface perfection.

ments. A uniform adjustment of absolute values of about 40% will cause Allen and Gobeli's data and ours to match above ~5.3 eV and our lower energy yields will then fall between their upper and lower limits. Such a difference is well within experimental error since they estimate theirs to be "probably correct to within a factor of 2." Thus a considerable similarity has been established between silicon surfaces prepared by proper polishing and annealing and those prepared by cleaving and annealing.

IV. PHOTOELECTRIC YIELD—RESULTS ON GOOD SURFACES

A. Clean Surfaces

The photoelectric yield spectra are shown in Fig. 2 for four different surfaces of single crystal silicon as obtained by the improved system described above. All were prepared by chemical-mechanical polishing and annealing for one to several hours at 850°C in vacuum of $\sim 1\times 10^{-10}$ Torr. All surfaces gave excellent LEED patterns corresponding to their orientation, such as published in the literature.[10] Surfaces A and A' are oriented (111), B is (110), and C is (100), all within $\pm 1°$. Although the data shown are those for specific samples, they were repeated for at least three samples of each orientation. There was some variability in the low-energy yields from sample-to-sample. The majority of low-energy curves fell on that shown by A, Fig. 2. The remainder (for properly annealed samples) were observed to vary between A and A'; these were found to be unstable and are not used in the analysis.

B. Surfaces Exposed to Oxygen

Crystallographic differences in yields can be due either to differences in barrier heights or band structures. By performing experiments which change only barrier heights, it is possible to distinguish between these alternatives. Either barriers can be lowered (as often done by the application of cesium) or they can be raised. The latter procedure was employed here by adding controlled amounts of oxygen.

Hence, photoelectric yield spectra were obtained for samples of (111), (110), and (100) silicon which were exposed to oxygen in the amount of some 10^{-6} Torr sec as shown in Fig. 3. Exposures were regulated so that the yield for the exposed (110) sample ($Y_{110}{}^{x}$) were identical at one energy (5.6 eV). In addition, the aim was to decrease the work function of (111) and (110) by regulating $Y_{111}{}^{x}$ and $Y_{110}{}^{x}$ to become equal to the yield for the unexposed (100) sample (Y_{100}) at one energy—it can be seen that the exposure was not quite sufficient to accomplish this, but the essential information has been obtained. Also, in order to check that important features of the yields do not vary with these small changes in barrier height, yields, as shown in Fig. 3, were obtained for (100) surfaces exposed to oxygen.

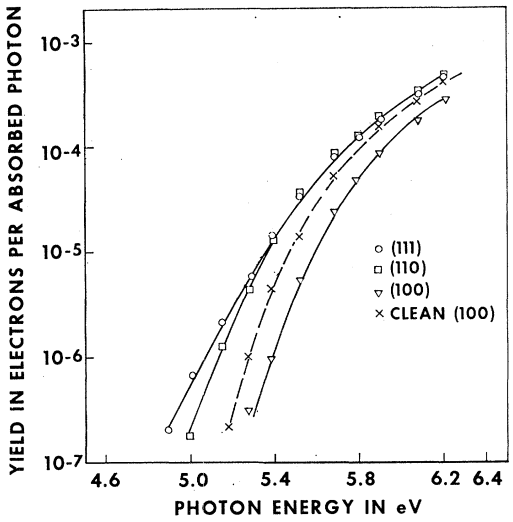

FIG. 3. Photoelectric yield curves for (111), (110), and (100) exposed to oxygen in order to raise barrier heights.

It is interesting to note that the analysis to follow indicates that the operant optical transitions occur in regions of the band structure for which dE/dk is much greater in conduction than valence band. Hence, variations in $h\nu$ should be almost equivalent to variations in barrier height. Thus, it turns out that this information could have also been obtained, and consistency requires that it be so, simply by shifting the curves in Fig. 2 along the abscissa. Such procedure might even be expected to be more accurate since no modification of the surface is required. When this is done, one indeed confirms the results from oxidized surfaces. Moreover, it is found (as it should be) that the distance which the curves must be shifted in $h\nu$ to match curves at higher energies, agrees with differences in ξ obtained from work function data[4]; i.e., one finds $\xi_{111}=\xi_{110}$ (no shift required) and $\xi_{100}=\xi_{111}+0.18$ eV ± 0.02 eV.

C. Important Features of Experimental Results

(1) Y_{111} and Y_{110} are identical for optical energies $\gtrsim 0.8$ eV above the threshold, but diverge below.

(2) Although oxygen exposure was not quite sufficient it appears clear that $Y_{111}{}^{x}\cong Y_{100}$ for optical energies $\gtrsim 1.0$ eV above the (111) threshold and they diverge at lower energies. This is verified by the results of the curve shifting procedures.

(3) At lower optical energies $Y_{111}>Y_{110}>Y_{100}$.

V. INTERPRETATION OF RESULTS

A. Transport Effects

In the optical energy range from ~4.5 to 6.5 eV, it is reasonable to expect, and generally assumed,[1–3,5] that

[10] F. Jona, IBM J. Res. Dev. 9, 375 (1965).

photoelectric yields from clean silicon are mainly due to electrons which are not scattered before they arrive at the surface. Electron-electron scattering can probably be neglected since it has been shown both theoretically[11] and experimentally[12] that the mean free path for pair production is about 180 Å, which is considerably greater than the optical absorption depth of 60 Å (as computed from reflectivity data[6]). Phonon interactions are not likely to predominate since it has been shown that a large fraction of photoemitted electrons emerge with no change in crystal momentum[13]; this is consistent with an estimate[12] of 60 Å for the mean free path (which could actually be larger) for phonon scattering. However, at energies lower than those considered here, the optical-absorption depth increases greatly and phonon scattering becomes more important.

In the analysis to follow, it turns out that the principal features of observed yields can indeed be explained over the full energy range without considering scattering.

B. Threshold Energies

Photoelectric yield data are often expressed[2] as power laws in photon energy $h\nu$, the yield Y being given as

$$Y \propto (h\nu - h\nu_0)^n, \tag{1}$$

where $h\nu_0$, the threshold energy, and the exponent n are determined by matching with experiment. This has been done either empirically or in order to make comparisons with theory, most recently that of Kane,[14] which predicts that, *near threshold*, Eq. (1) holds with n ranging from 1–$\frac{5}{2}$, depending on the production and scattering mechanisms. van Laar and Scheer[15] were able to match their data on cleaved-in-vacuum unannealed silicon by the expression

$$Y = C_1(h\nu - 4.85)^{5/2} + C_2(h\nu - 5.40)^{3/2}, \tag{2}$$

with $C_2/C_1 = 28.5$. For similar surfaces, of higher perfection, Gobeli and Allen[16] used the relation

$$Y = C_1(h\nu - 5.15)^{5/2} + C_2(h\nu - 5.45). \tag{3}$$

On cleaved-and-annealed silicon, Gobeli and Allen[5] described their results with the expression

$$Y = C_1(h\nu - 4.55)^2 + C_2(h\nu - 5.3). \tag{4}$$

The second terms in (2) to (4) were associated with direct transitions from the valence band by both groups, as predicted by Kane[14] for a linear exponent whereas the first terms were ascribed to surface states by van Laar and Scheer[15] and to phonon assisted indirect transitions by Gobeli and Allen.[16] Subsequently it was pointed out by Gobeli and Allen[17] that their experiments with polarized light[13] rule out indirect transitions; they believe also that negligible emission from surface states is observed for several reasons, mainly associated with evidence that all photoelectrons are produced beneath the surface.[17,18] Moreover, yields near threshold in InAs have been identified[19] with direct transitions. However, Fischer[20] has shown that observed yield spectra of many materials cannot be explained by simple superposition, such as shown in Eqs. (2)–(4); he suggests that "the transition from one yield law to the other is connected with the optical excitation mechanism or details of the band structure."

We have found it impossible to fit the data presented in Fig. 2 to a single or double power-law expression over the whole energy range in a convincing manner. Moreover, as mentioned previously, we found that because of the improved high energy data of Fig. 2, the linear dependence of Fig. 1 above ~5.6 eV (which was also observed by Gobeli and Allen and ascribed to a direct process[5]) no longer is seen.

The resolution of these inconsistencies lies in the appreciation that Kane's theory has been used beyond its region of applicability. The theory[14] is derived only for small $\mathbf{k}-\mathbf{k}_d$, where $\mathbf{k}_d$ is the value of crystal momentum, $\mathbf{k}$, at threshold. And the analysis to follow (see Sec. VII) shows that, for clean silicon, $\mathbf{k}-\mathbf{k}_d$ becomes large for $(h\nu - h\nu_0)$ less than ~0.2 eV. Thus, only *one mechanism* is required to explain all results, and that is *direct transitions* from valence to conduction band. Hence, there is only *a single threshold* which properly must be determined by matching observed yields to a linear exponent only for a small range in $(h\nu - h\nu_0)$. Using this procedure, we find

$$E_t(111) = 4.60 \text{ eV}; \quad E_t(110) = 4.73 \text{ eV}; \quad E_t(100) = 5.11 \text{ eV}. \tag{5}$$

Accuracies are ±0.03 eV.

C. Crystallographic Dependence of Yield at Lower Energies

Figure 4 shows the band structure for silicon determined by Cohen and Bergstresser[21] along symmetry directions Λ, Δ, and Σ (which are along ⟨111⟩, ⟨100⟩, and

[11] E. O. Kane, Phys. Rev. **159**, 624 (1967).
[12] D. J. Bartelink, J. L. Moll, and N. I. Meyer, Phys. Rev. **130**, 972 (1963).
[13] G. W. Gobeli, F. G. Allen, and E. O. Kane, Phys. Rev. Letters **12**, 94 (1964).
[14] E. O. Kane, Phys. Rev. **121**, 131 (1962).
[15] J. van Laar and J. J. Scheer, in *Proceedings of the International Conference on the Physics of Semiconductors, Exeter* (Adlard and Sons, Ltd. Bartholomew Press, Dorking, England, 1962), p. 827.
[16] G. W. Gobeli and F. G. Allen, Phys. Rev. **127**, 141 (1962).
[17] G. W. Gobeli and F. G. Allen, Phys. Rev. **137**, A245 (1965).
[18] G. W. Gobeli, E. O. Kane, and F. G. Allen, in *Optical Properties and Electronic Structure of Metals and Alloys* (North-Holland Publishing Co., Amsterdam, 1966), p. 348.
[19] T. E. Fischer, F. G. Allen, and G. W. Gobeli, Phys. Rev. **163**, 703 (1967).
[20] T. E. Fischer, Phys. Rev. **142**, 519 (1966).
[21] M. L. Cohen and T. K. Bergstresser, Phys. Rev. **141**, 789 (1966).

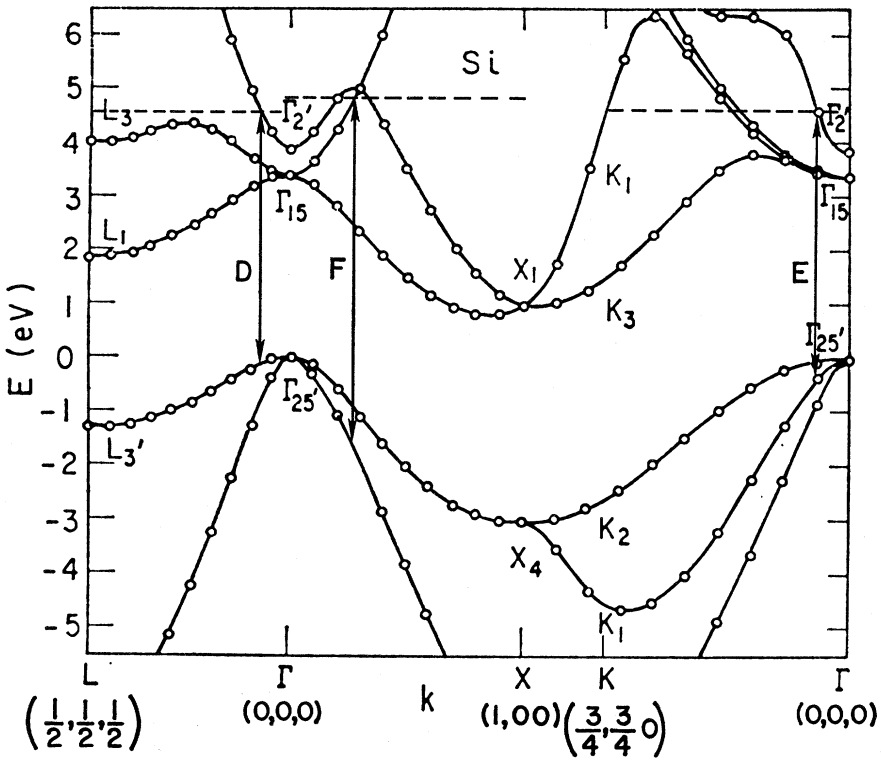

FIG. 4. Silicon band structure determined by Cohen and Bergstresser (Ref. 21). Possible transitions to vacuum level at dashed lines identified by *D*, *E*, *F*. The dashed lines indicate the potential barrier at the surfaces as indicated. (These surfaces are ⊥ to the respective **k** vectors.)

⟨110⟩, respectively) and from *X* to *K*. Other calculations[22–24] (which also determine lower level conduction bands throughout the zone) have given similar results in the region of interest. We have placed dashed lines at the vacuum energy levels [determined from the (111) threshold and contact potential differences[4]] and have drawn arrows representing threshold optical energies for transitions which have **k** along the three symmetry directions. Transitions only between wavefunctions of the proper symmetries are permitted.[25]

It can be seen at once that the experimental *trend* of E_t versus crystal orientation shown in expression (5) follows the indication of Fig. 4. The optical energy needed for emission to the vacuum level of electrons ⊥ the surfaces increases for transitions with k along ⟨111⟩, ⟨110⟩, and ⟨100⟩, respectively. However, the magnitudes of the experimental energy differences are smaller than predicted. The length of arrows *D*, *E*, and *F* in Fig. 4 predicts that at threshold for *normal* electrons $E_t(110)-E_t(111)\simeq 0.3$ eV and $E_t(100)-E_t(111)\simeq 1.7$ eV, whereas experimental differences = 0.13 and 0.5 eV, respectively. Thus observed yield cannot be due to electrons with $\mathbf{k}\perp$ the surfaces. Note that the rapid decrease in valence band energy for increasing $|\mathbf{k}|$ leads to even greater discrepancies with increasing $(h\nu-h\nu_0)$.

[22] D. Brust, Phys. Rev. **134**, A1337 (1964).
[23] E. O. Kane, Phys. Rev. **146**, 558 (1966).
[24] L. R. Saravia and D. Brust, Phys. Rev. **171**, 916 (1968).
[25] B. S. Gourary (private communication).

D. Higher-Energy Yields

The identity of the yield spectra at higher energies for (111) and (110) and the near identity for (100) and oxidized (111) indicate strongly that the observed photoelectrons originate from *identical* optical transitions. (A corollary of this observation is that, as found by Allen,[4] $\xi_{111}=\xi_{110}$, and $\xi_{110}<\xi_{100}$.)

Now, considering only vertical transitions, the photoelectric yield is given by[14,22,26]

$$Y(h\nu)=\sum_{n,s}\int_{BZ}|\mathbf{A}\cdot\mathbf{P}_{n,s}|^2P(E_n,\mathbf{k})\times\delta[E_n(\mathbf{k})-E_s(\mathbf{k})-h\nu]d^3\mathbf{k}\Big/\sum_{n,s}\int_{BZ}|\mathbf{A}\cdot\mathbf{P}_{n,s}|^2\times\delta[E_n(\mathbf{k})-E_s(\mathbf{k})-h\nu]d^3\mathbf{k}. \quad (6)$$

Transitions occur between pairs of bands with conduction bands indexed by n and valence bands by s. $|\mathbf{A}\cdot\mathbf{P}_{ns}|^2$ is the dipole matrix element connecting the bands, and **A** is the vector potential of the light. The integral extends over the Brillouin zone (BZ). $P(E_n,\mathbf{k})$ is the probability that an electron with energy E_n and crystal momentum **k** will escape.

The optical transitions responsible for observed yields are determined by surface orientation in two ways:

[26] D. Brust, Phys. Rev. **139**, A489 (1965).

(1) Escape is limited to those electrons which satisfy conservation requirements. These depend on $\mathbf{k}$ (see Sec. VI). (2) Transitions are excited only for $\mathbf{A}$ in the plane $\perp$ the surface normal, since the experiments are performed at normal incidence. Thus, it would be expected that yields should be strongly dependent on crystalline orientation, but the experimental results indicate otherwise at higher energies. To explain this result, we begin with the calculation in Sec. VI.

VI. ANALYSIS

A. Emission of Non-normal Electrons

Since the previous considerations suggest strongly that observed yields are due to non-normal electrons, we wish to determine the additional optical energy required to emit electrons at threshold with k at the angle θ to $\hat{n}$, the surface normal. This energy must be equal to the tangential energy in the vacuum at threshold. Let $\mathbf{k}_{11}{}^{i}$ and $\mathbf{k}_{11}{}^{0}$ be the components of $\mathbf{k}$ parallel to the surface, inside and outside the crystal, respectively, $\mathbf{k}_{11}{}^{0}$ being electron momentum and $\mathbf{k}_{11}{}^{i}$ crystal momentum. Conservation of parallel momentum across the boundary is given by $\mathbf{k}_{11}{}^{0}=\mathbf{k}_{11}{}^{i}+\mathbf{K}$, where $\mathbf{K}$ is a vector of the reciprocal lattice[27]; since we are interested in the lowest energy threshold, only $\mathbf{K}=0$ need be considered. Hence, we find

$$E_A=E_p=[(\hbar\mathbf{k}_{11}{}^{0})^2/2m]=[(\hbar\mathbf{k}_{11}{}^{i})^2/2m], \qquad (7)$$

where E_A is the additional threshold energy required which must be equal to E_p, the energy of the electron with $\mathbf{k}_{11}{}^{0}$, in the vacuum (thus m is the free-electron mass). Expressing in terms of θ, Eq. (7) becomes

$$E_A=E_{\mathrm{BZ}}f^2\sin^2\theta, \qquad (8)$$

where $f(=|\mathbf{k}|/|\mathbf{k}_e|)$ is the ratio of the magnitude of $\mathbf{k}$ to its value at the edge of the Brillouin zone (BZ); $|\mathbf{k}_e|=(2\pi/a)(\frac{1}{2},\frac{1}{2},\frac{1}{2})$. $E_{\mathrm{BZ}}(=\hbar^2k^2/2m)$, the energy at the edge of the zone, $=4.0$, 3.5, and 4.6 eV for $\mathbf{k}$ in the direction $\langle 111\rangle$, $\langle 110\rangle$, or $\langle 100\rangle$, respectively.

B. Origin of High-Energy Yields

Setting $\theta=90°$ in Eq. (8) shows that $E_A\leq f^2E_{\mathrm{BZ}}$ is required to emit electrons at any direction of $\mathbf{k}$, and if the operant transitions are not too far from the zone center, as suggested by Fig. 4, E_A can be quite small.

The most plausible explanation of the identical yields in light of the above considerations is that the transitions responsible are *all* possible transitions throughout the zone which terminate above the vacuum level; i.e., if sufficient optical energy is available electrons will escape for all $\mathbf{k}$. Yields (as observed) are expected to be isotropic and independent of the direction of A,[28] since silicon is cubic.

C. Position of Transitions Throughout Brillouin Zone

Using the above calculations and our interpretation of high-energy yields, the distance from the center of the zone of transitions responsible for observed yields (f_y) can be estimated. The experimental data show that $h\nu-h\nu_0\geq 1.0$ eV is sufficient to excite transitions for all directions of $\mathbf{k}$. Using this information, f_y turns out to be about 0.5 or less. Thus there must be few high probability transitions in the outer part of the zone above the vacuum level.

D. A Comparison with Experiment

Since details of the band structure throughout the zone for energies between 4.6 and 6.5 eV appear in the literature only for symmetry directions, a close quantitative comparison with experiment is not feasible. However, an examination of Fig. 4 suggests an explanation which leads to reasonable agreement with experiment. Notice that the threshold energy is somewhat lower along $\langle 111\rangle$ and that only for the $\langle 111\rangle$ direction do the transitions allowed by symmetry of the wave functions originate in the upper valence band. Therefore, it is likely that the majority of observed photoelectrons *near threshold* could come from transitions with $\mathbf{k}$ near the $\langle 111\rangle$ direction. The possibility cannot be ruled out, of course, that electrons emerge normally from off-symmetry directions.

The disposition of $\langle 111\rangle$ directions for (100), (110), and (111) surfaces is shown in Fig. 5. In order to relate theory and experiment, yields from $\mathbf{k}$ at only a single $\langle 111\rangle$ must be considered. Hence experimental yields Y_{111}, $\frac{1}{2}Y_{110}$, and $\frac{1}{4}Y_{100}$ were obtained from Fig. 2 (correcting for variation in ξ as in Sec. IV B) and have been plotted in Fig. 6. The quantity f is here treated as a parameter (f') to be determined by matching of theory and experiment. Figure 6 shows that the thresholds for emission with $\mathbf{k}$ at a *single* $\langle 111\rangle$ direction from a (110) and a (100) surface are 0.16 and 0.37 eV higher than for (111). According to our model, these additional photon energies are required to provide the minimum amount of tangential momentum for escape (see Fig. 5). The parameter f', as determined from Eq. (8), is found to be 0.35 for the (110) surface and 0.37 for the (100) surface; which is indeed consistent with transitions not far from the zone center, as suggested by Fig. 4.

E. Speculation

In light of the above discussion it can be speculated that variations in yield very close to threshold observed here and elsewhere have been at least partly due to electrons scattered into states with small $\mathbf{k}$ by samples

[27] Parallel momentum conservation is proved merely by the existence of good LEED patterns at low primary energies. We are indebted to P. E. Best for this observation.

[28] P. N. Butcher, Proc. Phys. Soc. (London) **A64**, 765 (1951).

with surface irregularities. For the (111) surface, scattering would be out of states along the three ⟨111⟩ directions at an angle of 71° to the surface normal.

VII. ENERGY DEPENDENCE OF YIELD

The considerations on crystallographic probability of emission have necessary consequences for energy dependence of yields and lead to an interpretation which is different than heretofore proposed, but which is a logical extension of the suggestion of Fischer[19] (see Sec. V B). Only a single mechanism is required: i.e., direct optical excitations; of course other possibilities are not ruled out in general.

We view the yield in three regions: (1a) The near-threshold region, which is defined as that for which

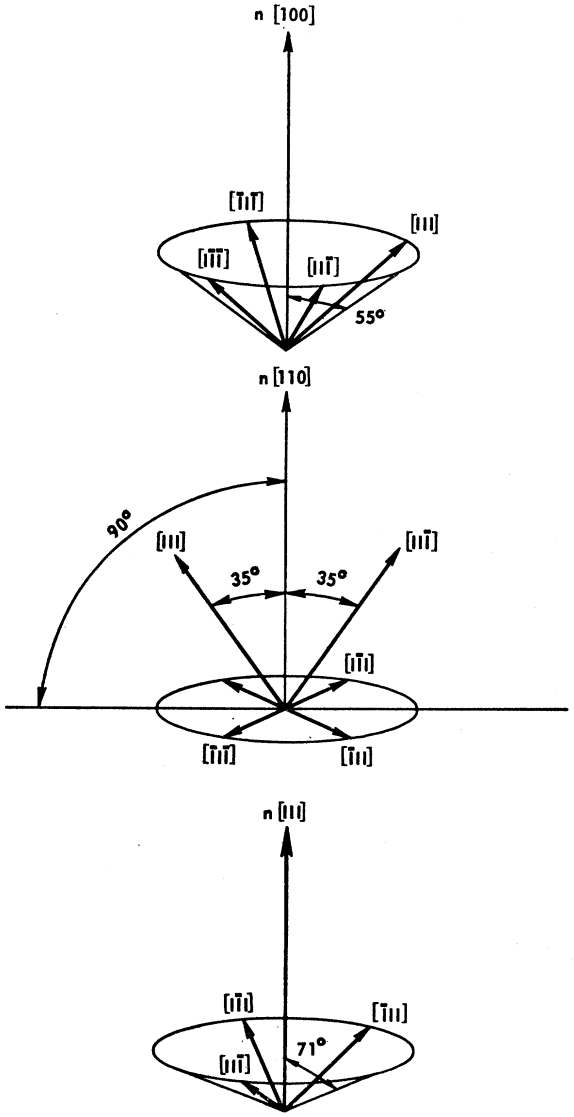

FIG. 5. Disposition of ⟨111⟩ directions for (100), (110), and (111) surfaces.

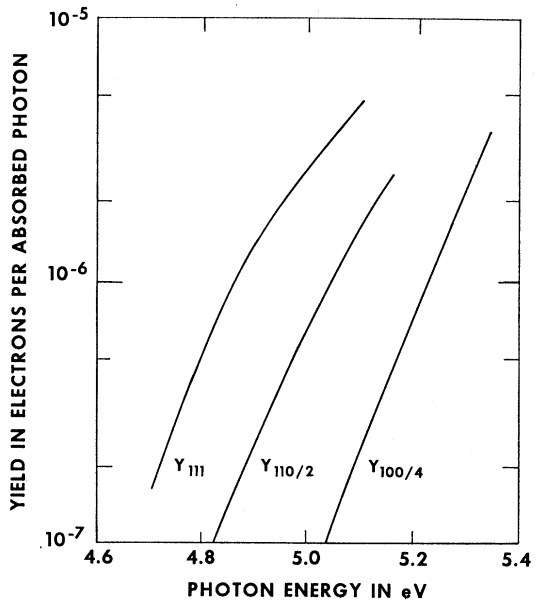

FIG. 6. Yield from (111); ½ yield from (110); ¼ yield from (100) calculated from Fig. 3 near threshold for comparison with theory.

$\mathbf{k}-\mathbf{k}_d$ is small, as treated by Kane[13]; this is really a subregion of the next stage since the same mechanism occurs but $(h\nu-h\nu_0)$ is small. (1) The escape angle region, for which $\mathbf{k}-\mathbf{k}_d$, and thus θ, become larger with increasing photon energy. Further increase in $(h\nu-h\nu_0)$ leads to (2) the optical excitation region for which the escape angle $\theta=90°$ so that all electrons excited above the vacuum level are emitted; yields are determined only by transition probabilities and densities of state.

The range of applicability of $(h\nu-h\nu_0)$ to (1a) can be estimated by letting $\theta=30°$ as an upper limit in Eq. (8) so that $|\mathbf{k}-\mathbf{k}_d|=\frac{1}{2}k_d$, which is thus no longer small; using 0.35 for f as found above, we find $E_A=0.12$ eV. Moreover, the energy at which region (2) begins is known since it was found that $\theta=90°$ for $(h\nu-h\nu_0)$ greater than 1.0 eV.

Thus we conclude that for clean silicon in the observed range: Y is in region (1a) for $(h\nu-h\nu_0)\lesssim 0.2$ eV, region (1) for 0.2 eV $\lesssim(h\nu-h\nu_0)\gtrsim 1.0$ eV, and region (2) for $(h\nu-h\nu_0)\gtrsim 1$ eV; hence all regions are accessible over the observed range in $h\nu$.

This explanation can be described in terms of Eq. (6) for which the escape function P can be written

$$P(E,\mathbf{k})=S(E_n-E_0-E_A)$$
$$=S(E_n-E_0-f^2E_{BZ}[\mathbf{k}\times\hat{n}]^2), \quad (9)$$

where Eq. (8) has been used for E_A; and where $S(X)$ is a step function so that

$$S(x)=0, \quad x\leq 0, \quad S(x)=1, \quad x\geq 0, \quad (10)$$

which specifies that if the electron is excited to a sufficiently high energy it will escape, otherwise it will

not. Neglecting the dependence of $|\mathbf{A}\cdot\mathbf{P}_{ns}|^2$ on $\mathbf{k}$ (which has been found to be a satisfactory approximation at lower band energies[22]), Y can be written using Eqs. (6) and (9):

$$Y(h\nu,E_0)=\sum_{n,s}\int_{BZ} S[E_n(\mathbf{k})-E_A(\mathbf{k})-E_0] \times\delta[E_n(\mathbf{k})-E_s(\mathbf{k})-h\nu]d^3\mathbf{k} \Big/ \sum_{n,s}\int_{BZ}\delta[E_n(\mathbf{k})-E_s(\mathbf{k})-h\nu]d^3\mathbf{k}.$$

In the near-threshold region (1a) $h\nu$ is just large enough that the δ function in the integral picks out transitions for which E_n just exceeds E_0+E_A. In region (1) sufficient optical energy is available so that increasingly large numbers of the transitions (for given indices n and s) have $E_n>E_0+E_A$ as $h\nu$ increases and θ becomes even larger until in region (2) the large majority of transitions terminate above the step function; thus $\theta=90°$.

For the proper interpretation of photoemission results, including both yield and energy distribution measurements, considerations such as those reported here must be taken into account; i.e., the effect of the $\mathbf{k}$ vector of the transitions on the emission probability must be considered. Structure in energy distributions which appear with increasing photon energy can be due to accessibility for emission of electrons from transitions further out in the zone as well as to accessibility for excitation at higher energies (as generally considered); such effects can be significant for energies at least up to E_{BZ}.

VIII. SUMMARY AND CONCLUSIONS

It was established that the spectral photoelectric yield for properly polished and annealed (111) silicon is the same as that of cleaved and annealed silicon.

Photoelectric yields (Y) were obtained for (111), (110), and (100) silicon surfaces. After eliminating effects due to surface barrier differences, it was found that for photon energies up to $\sim$1 eV above threshold [i.e., $(h\nu-h\nu_0)\lesssim 1$ eV], $Y_{111}>Y_{110}>Y_{100}$; whereas for $(h\nu-h\nu_0)\gtrsim 1$ eV, $Y_{111}=Y_{110}=Y_{100}$.

Improved experimental conditions showed that higher energy yields for (111) increase more rapidly with $(h\nu-h\nu_0)$ than previously observed.

Using the interpretation and analysis below, some previous inconsistencies in finding thresholds were resolved by showing that the threshold region of the theory[14] applies only for $(h\nu-h\nu_0)\lesssim 0.2$ eV, and only a single mechanism is required (i.e., direct excitation). Thresholds determined on this basis are 4.60 eV for (111), 4.73 eV for (110) and 5.11 eV for (100), $\pm$0.03 eV.

Using known band structure calculations along symmetry directions, it can be seen (Fig. 4) that there are no available transitions with $\mathbf{k}\perp$ to (110) and (100) surfaces, hence observed yields are due to non-normal electrons. Therefore, the energy above threshold, E_A, required for emission of electrons with $\mathbf{k}$ at the angle θ to the surface normal was calculated. The results showed that θ can become quite large ($\sim$30°) for $(h\nu-h\nu_0)$ only a few tenths of an eV; θ increases with $(h\nu-h\nu_0)$ until it becomes $=90°$ for $(h\nu-h\nu_0)\gtrsim 1.0$ eV. Thus a new interpretation of versus $(h\nu-h\nu_0)$ is involved. Three regions occur: (1a) the near-threshold region for small θ; (1) the escape angle or partial escape region; and (2) the complete escape region for which sufficient optical energy is available to emit all electrons which reach the surface above the vacuum level. The observed identical yields at higher energies occur because region (2) applies.

A quantitative estimate of *lower-energy* crystallographic differences in yields was made on the assumption, suggested by examination of Fig. 4, that the transitions are peaked for k along $\langle 111\rangle$—good agreement with experiment was obtained.

For any material, the energy range of each stage is determined by the position in the Brillouin Zone of the operant optical transitions. Proper interpretation of photoemission results, including both yield and energy distribution measurements require that such factors be considered.

ACKNOWLEDGMENTS

The author would like to thank Dr. P. E. Best and Dr. H. C. Abbink for helpful discussions, Dr. G. A. Peterson for critical reading of the manuscript, and to express his appreciation for the assistance of V. Failla, who aided in design and construction, operated the apparatus, and took most of the data.